ON FABRICATION OF NANOSCALE NON-SMOOTH FIBERS WITH HIGH GEOMETRIC POTENTIAL AND NANOPARTICLE'S NON-LINEAR VIBRATION

by

Xin YAO[a] and Ji-Huan HE[a,b*]

[a] National Engineering Laboratory for Modern Silk, College of Textile and Clothing Engineering, Soochow University, Suzhou, China
[b] School of Mathematics and Information Science, Henan Polytechnic University, Jiaozuo, China

Original scientific paper
https://doi.org/10.2298/TSCI2004491Y

Non-smooth surface of a nano or micro-scale fiber has an extremely large surface area and a tremendously high surface energy (geometric potential). This paper focuses on the formation mechanism of fabrication of a non-smooth surface by electrospinning through controlling solvent evaporation and nanoscale adhesion of nanoparticles on the surface. Poly(vinylidene fluoride), multi-wall carbon nanotubes and a binary solvent system are adopted in the experiment to elucidate how to fabricate nanoscale porous nanofibers and lotus-surface-like nanofibers. A nanoparticle's vibration near its equilibrium is also discussed, which also affects greatly the surface morphology.

Key words: *lotus effect, antifouling, self-cleaning, Bernoulli equation, non-linear oscillation, frequency-amplitude relationship*

Introduction

Nanofibers have a large surface area, which produces a high geometric potential (surface energy) [1-7], as a result, nanofibers can find wide applications in various areas. If we want to have an even higher surface energy for an advanced application, smaller nanofibers are needed, but its fabrication process becomes impossible when fiber diameter reaches a threshold, and its cost becomes higher. So we should search for fabrication processes to remarkably increase fiber's surface area, among which the nanoscale porous fibers [8-12] have been caught much attention, Liu *et al.* [13] used a multiple solvent system to control the solvent evaporation to fabricate controllable nanoporous fibers. Zhao *et al.* [14] found that the sudden solvent evaporation was an efficient way to produce nanoporous fibers. Peng *et al.* [15] suggested a Rachford-Rice-like equation for estimation of solvent evaporation. The solvent's fast evaporation always results in a porous fiber with a concave surface during the electrospinning process. In this paper we will try to fabricate lotus-surface-like nanofibers with convex surface

Experimental design

Poly(vinylidene fluoride) (PVDF), and multi-wall carbon nanotubes (MWCNT) with diameter ranging from 10 nm to 20 nm and length ranging from 30 μm to 100 μm) were

* Corresponding author, e-mail: hejihuan@suda.edu.cn

used in our experiment. A binary solvent system was prepared using N,N-dimethylformamide (DMF) and acetone with 7:3 mole ratio, and a 10% PVDF solution was prepared as a similar way in our previous publications [16-19]. In order to study the effect of MWCNT on the surface property of nanofiber, 0.5 wt.% MWNT were added to the 10% PVDF solution.

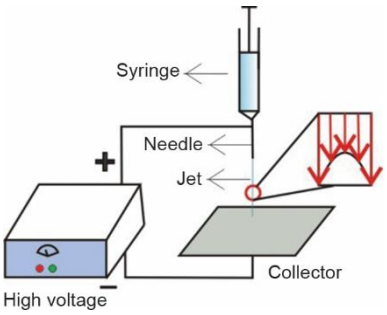

Figure 1. Experimental set-up

The experimental set-up was illustrated in fig. 1, the solution was placed into a 10 mL plastic syringe installed with a stainless steel-needle as the spinneret. The plastic syringe was connected to a 20 KV voltage source while a collector was grounded. The distance between the needle tip and the collector was 18 cm for PVDF solution and 15 cm for PVDF/MWNT solution, respectively. The feeding rate of the solution in the syringe was controlled at 1.0 mL/h.

Surface morphologies of PVDF fibers and PVDF/MWCNT fibers were given, respectively, in figs. 2 and 3. The surface of pure PVDF fiber is porous, while that of PVDF/MWCNT is lotus-surface-like structure with nanoparticles on the surface. The binary solvent system was discussed in [14], where the formation mechanism of nanoscale porous surface was also elucidated. The fast solvent evaporation is the key factor for fabricating nanoscale porous fibers. During the spinning process, a moving jet becomes gradually solidified, while the solvent evaporation can effectively control the solidification process, smooth and small fibers can be obtained when the solvent evaporation is slow. However, when some a solvent in the binary solvent system, *e. g.*, acetone, has a faster evaporation ratio, nanoscale porous fibers with larger diameter are predicted.

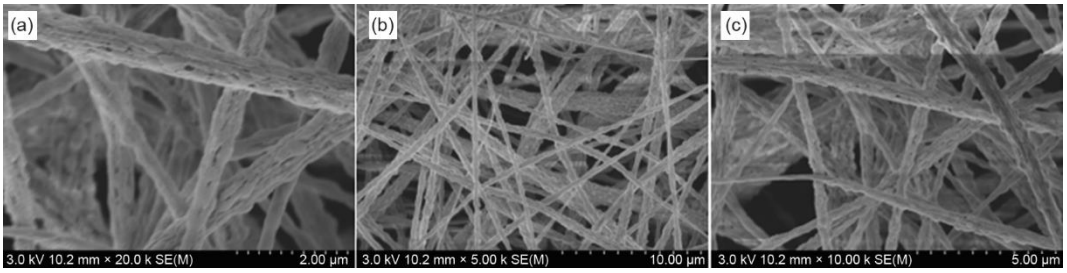

Figure 2. The SEM images of unsmooth PVDF fibers with average fiber diameter of 396±79 nm

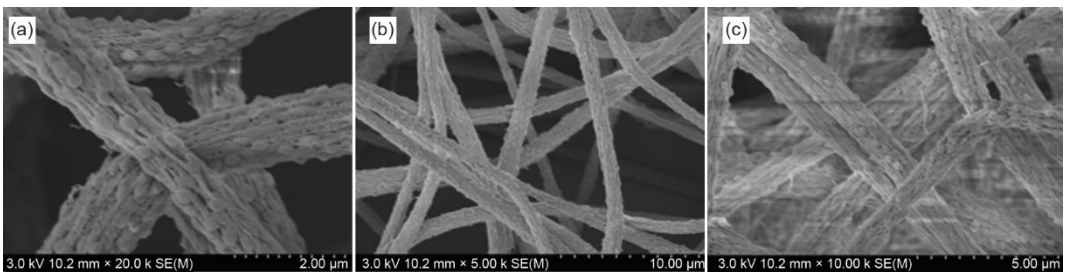

Figure 3. The SEM images of unsmooth PVDF/MWNT fibers with average fiber diameter of 1220±286 nm), the average size of the nanoparticles on the surface is 293±39 nm X 180±45 nm

Theoretical analysis

Fiber diameter can be predicted by the mass equation of 1-D fluid:

$$\pi r^2 \rho u = Q \tag{1}$$

where r is the radius of the moving jet, u – the velocity, ρ – the density, and Q – the flow ratio, which is a constant in our experiment.

For the PVDF/MWNT solution, the section area of the jet can be written in the form:

$$\pi r^2 = A_{\text{PVDF}} + A_{\text{MWNT}} \tag{2}$$

where A_{MWNT} and A_{PVDF} are section areas occupied by the PVDF solution and MWNT particles, respectively. During the spinning process A_{MWNT} keeps unchanged as shown in fig. 4. So we can predict a larger fiber size of the PVDF/MWNT fibers than that of PVDF fibers.

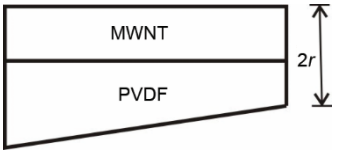

Figure 4. The spinning process of PVDF/MWNT jet

The PVDF/MWNT jet has higher viscous force than that of the PVDF jet, the MWNT particles hinder the fluid, so we need a higher force in the spinning process. In our experiment, we shorten collector's distance from 18 cm to 15 cm.

In order to elucidate the surface morphology of PVDF/MWNT fibers. We consider Bernoulli equation:

$$\frac{1}{2}u^2 + \frac{P}{\rho} = \text{B} \tag{3}$$

where P is the pressure and B – the Bernoulli constant.

Tian *et al.* [20-22] suggested a macromolecular electrospinning using a long and narrow tube, so that macromolecule orientation can be easily controlled by the Bernoulli equation. The same principle can be also applied to control the nanoparticles distribution. We assume that nanoparticles are distributed uniformly on the section of the spinneret as illustrated in fig. 5. As the electrostatic force acts on the surface of the moving jet, the velocity distribution is not as that in a tube flow. The velocity is maximal on the surface of the boundary, and it is minimal in the center of the jet, fig. 5.

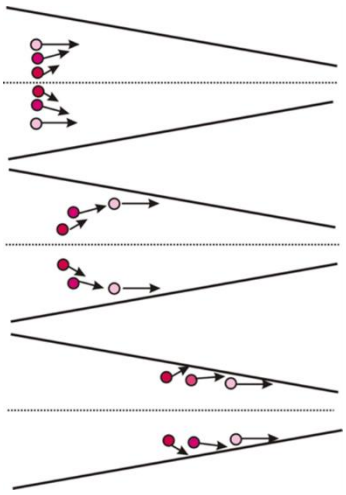

Figure 5. Velocity distribution and particle motion in the moving jet

Considering two points on the section of the moving jet, one is at the center, the other is on the boundary, according to the Bernoulli equation, there exists a pressure gradient, which is:

$$P_{\text{center}} - P_{\text{boundary}} = \frac{1}{2}\left[\rho(u_{\text{boundary}})^2 - (u_{\text{center}})^2\right] > 0 \tag{4}$$

This pressure gradient is the acting force that pushes gradually the particles in the center to the boundary, and finally all particles will be all distributed on the surface.

According to MWNT producer, MWNT are nanofibers with diameter ranging from 10 nm to 20 nm and length ranging from 30 μm to 100 μm, see the producer label in fig. 6.

Figure 6. Producer label describing MWNT properties

According to our experimental observation given in fig. 3, the used MWNT should have particle-like geometry with length of 293±39 nm and width of 180±45 nm.

Particle oscillation

When a particle moves onto the surface of the moving jet, a small perturbation will arouse its vibration. We assume that the particle moves a distance radially from the boundary to the center, due to the pressure difference, the particle will push back to its equilibrium position, the force can be expressed:

$$F = A\frac{\Delta P}{\Delta x} \tag{5}$$

where A is section area of the particle. Ignoring the viscous force, we have the following motion equation:

$$F = m\ddot{x} \tag{6}$$

where m is the mass of the particle and x – the radial co-ordinate. We assume the velocity distribution has the form:

$$u = u_0 + \frac{u_b - u_0}{r^2}x^2 \tag{7}$$

where u_0 and u_b are the velocities at the center ($x = 0$) and the boundary ($x = r$), respectively.

It is obvious that:

$$\Delta u = \frac{2(u_b - u_0)}{R^2}x\Delta x \tag{8}$$

According to eq. (3), we have:

$$\Delta P = -\rho u\Delta u = -\frac{2\rho(u_b - u_0)}{R^2}\left(u_0 + \frac{u_b - u_0}{R^2}x^2\right)x\Delta x \tag{9}$$

In view of eq. (9), we re-write eq. (6) in the form:

$$m\ddot{x} + A\frac{2\rho(u_b - u_0)}{R^2}\left(u_0 + \frac{u_b - u_0}{R^2}x^2\right)x = 0 \tag{10}$$

We re-write eq. (10) in the form:

$$\ddot{x} + \omega^2 x + \varepsilon x^3 = 0 \tag{11}$$

where

$$\omega^2 = \frac{2\rho A u_0(u_b - u_0)}{mR^2} \tag{12}$$

$$\varepsilon = \frac{2\rho A(u_b - u_0)^2}{mR^4} \tag{13}$$

Equation (11) is the well-known Duffing equation, it can be solved by the Taylor series method [23], the variational iteration method [24, 25], the variational method [26-29] and the homtopy perturbation method [30]. Here we use He's formulation [31, 32] to find the frequency-amplitude relationship:

$$\Omega^2 = \left.\frac{\mathrm{d}f(x)}{\mathrm{d}x}\right|_{x=A/2} = \left.(\omega^2 + 3\varepsilon x^2)\right|_{x=A/2} = \omega^2 + \frac{3}{4}\varepsilon A^2 \tag{14}$$

where Ω and A are the frequency and amplitude, respectively, $f(x)$ – the force, $f(x) = \omega^2 x + \varepsilon x^3$. In an energy form, eq. (11) can be deduced as a stationary condition of the following variational principle:

$$J(x) = \int_0^A \left[\frac{1}{2}\dot{x}^2 - \left(\frac{1}{2}\omega^2 x^2 + \frac{1}{4}\varepsilon x^4\right)\right]\mathrm{d}x \tag{15}$$

where $\dot{x}^2/2$ is the kinetic energy and $(\omega^2 x^2)/2 + (\varepsilon x^4)/4$ is the potential energy.

The oscillation of the nanoparticle on the boundary will greatly affect the surface morphology of the fibers.

Conclusions

This paper suggests two methods to fabricate unsmooth fibers, one is to use the multiple solvent system to fabricate porous fibers with concave surface, the other is to use nanoparticles as additives to fabricate lotus-surface-like nanofibers with convex surface. The unsmooth surface has many attractive properties, *e. g.*, antifouling, self-cleaning, superwettability, high surface energy (geometric potential). The Bernoulli equation is used to reveal the formation mechanism during the spinning process. Additionally this paper also suggests an experimental identification of the particle size by the solvothermal method [33] or the molecular beam method [34].

To exactly describe the jet motion during the spinning process, we need two-scale thermodynamics [35, 36], e. g., we need two scales to describe the spinning process. One scale is large where the Bernoulli equation or more accurately the laws in fluid mechanics works, and the other scale is much smaller, where the solvent evaporation should be considered, and fractal calculus [37-39] should be adopted.

Acknowledgments

The work is supported by Priority Academic Program Development of Jiangsu Higher Education Institutions (PAPD), National Natural Science Foundation of China under grant No. 11372205.

References

[1] Tian, D., *et al.*, Geometrical Potential and Nanofiber Membrane's Highly Selective Adsorption Property, *Adsorption Science & Technology, 37* (2019), 5-6, pp. 367-388
[2] Fan, J., *et al.*, Explanation of the Cell Orientation in a Nanofiber Membrane by the Geometric Potential Theory, *Results in Physics, 15* (2019), 102537
[3] Li, X. X., *et al.*, Nanoscale Adhesion and Attachment Oscillation Under the Geometric Potential, Part 1: The formation Mechanism of Nanofiber Membrane in the Electrospinning, *Results in Physics, 12* (2019), Mar., pp. 1405-1410
[4] Zhou, C. J., *et al.*, What Factors Affect Lotus Effect? *Thermal Science*, *22* (2018), 4, pp. 1737-1743

[5] Yang, Z. P., *et al.*, On the Cross-Section of Shaped Fibers in the Dry Spinning Process: Physical Explanation by the Geometric Potential Theory, *Results in Physics, 14* (2019), 102347
[6] Tian, D., Strength of Bubble Walls and the Hall-Petch Effect in Bubble-Spinning, *Textile Research Journal, 89* (2019), 7, pp. 1340-1344
[7] Tian, D., *et al.*, Hall-Petch Effect and Inverse Hall-Petch Effect: A Fractal Unification, *Fractals, 26* (2018), 6, 1850083
[8] Liu, Z., *et al.*, Humidity-Induced Porous Poly(Lactic Acid) Membrane with Enhanced Flux for Oil-Water Separation, *Adsorption Science & Technology, 37* (2019), 5-6, pp. 389-400
[9] Liu, L. G., *et al.*, Electrospun Polysulfone/Poly(Lactic Acid) Nanoporous Fibrous Mats for Oil Removal from Water, *Adsorption Science & Technology, 37* (2019), 5-6, pp. 438-450
[10] Li, Y., *et al.*, Glass Fiber Separator Coated by Porous Carbon Nanofiber Derived from Immiscible PAN/PMMA for High-Performance Lithium-Sulfur Batteries, *Journal of Membrane Science, 552* (2018), Apr., pp. 31-42
[11] Liu, F. J., *et al.*, Fabrication of Highly Oriented Nanoporous Fibers Via Airflow Bubble-Spinning, *Applied Surface Science, 421* (2017), Nov., pp. 61-67
[12] He, J. H., *et al.* Review on Fiber Morphology Obtained by Bubble Electrospinning and Blown Bubble Spinning, *Thermal Science, 16* (2012), 5, pp. 1263-1279
[13] Liu, L. G., *et al.*, Solvent Evaporation in a Binary Solvent System for Controllable Fabrication of Porous Fibers by Electrospinning, *Thermal Science, 21* (2017), 4, pp. 1821-1825
[14] Zhao, L., *et al.*, Sudden Solvent Evaporation in Bubble Electrospinning for Fabrication of Unsmooth Nanofibers, *Thermal Science, 21* (2017), 4, pp. 1827-1832
[15] Peng, N. B., *et al.*, A Rachford-Rice-Like Equation for Solvent Evaporation in the Bubble Electrospinning, *Thermal Science, 22* (2018), 4, pp. 1679-1683
[16] Zhou, C. J., *et al.*, Silkworm-Based Silk Fibers by Electrospinning, *Results in Physics, 15* (2019), Dec., 102646
[17] Zhao, J. H., *et al.*, Needle's Vibration in Needle-Disk Electrospinning Process: Theoretical Model and Experimental Verification, Journal of Low Frequency Noise, *Vibration and Active Control, 38* (2019), 3-4, pp. 1338-1344
[18] Liu, Z., *et al.*, Needle-disk Electrospinning Inspired by Natural Point Discharge, *Journal of Materials Science, 52* (2017), 4, pp. 1823-1830
[19] Li, Y., He, J. H., Fabrication and Characterization of ZrO_2 Nanofibers by Critical Bubble Electrospinning for High-Temperature-Resistant Adsorption and Separation, *Adsorption Science & Technology, 37* (2019), 5-6, pp. 425-437
[20] Tian, D., He, J. H., Macromolecular Electrospinning: Basic Concept & Preliminary Experiment, *Results in Physics, 11* (2018), Dec., pp. 740-742
[21] Tian, D., *et al.*, Macromolecule Orientation in Nanofibers, *Nanomaterials, 8* (2018), 11, 918
[22] Tian, D., *et al.*, Self-Assembly of Macromolecules in a Long and Narrow Tube, *Thermal Science, 22* (2018), 4, pp. 1659-1664
[23] He, J. H., Ji, F. Y., Taylor Series Solution for Lane-Emden Equation, *Journal of Mathematical Chemistry, 57* (2019), 8, pp. 1932-1934
[24] Anjum, N., He, J. H., Laplace Transform: Making the Variational Iteration Method Easier, *Applied Mathematics Letters, 92* (2019), June, pp. 134-138
[25] Nawaz, Y., *et al.*, An Effective Modification of He's Variational Approach to a Non-linear Oscillator, *Journal of Low Frequency Noise, Vibration and Active Control, 38* (2019), 3-4, pp. 1013-1022
[26] He, J. H., Sun, C., A Variational Principle for a Thin Film Equation, *Journal of Mathematical Chemistry. 57* (2019), 9, pp. 2075-2081
[27] He, J. H. A Modified Li-He's Variational Principle for Plasma, *International Journal of Numerical Methods for Heat and Fluid Flow*, On-line first, https://doi.org/10.1108/HFF-06-2019-0523, 2019
[28] He, J. H., Variational Principle for the Generalized KdV-Burgers Equation with Fractal Derivatives for Shallow Water Waves, *J. Appl. Comput. Mech., 6* (2020), 4, pp. 735-740
[29] He, J. H., Hamilton's Principle for Dynamical Elasticity, *Applied Mathematics Letters, 72* (2017), Oct., pp. 65-69
[30] Wu,Y., He, J. H., Homotopy Perturbation Method for Non-linear Oscillators with Co-ordinate Dependent mass, *Results in Physics, 10* (2018), Sept., pp. 270-271
[31] He, J. H., The Simplest Approach to Non-linear Oscillators, *Results in Physics, 15* (2019), 102546

[32] He, J. H., The Simpler, the Better: Analytical Methods for Non-linear Oscillators and Fractional Oscillators, *Journal of Low Frequency Noise, Vibration and Active Control, 38* (2019), 3-4, pp. 1252-1260
[33] Yang, F., Xue, M. Q., Facile Solvothermal Preparation and Tribological Performance of PbSe Nanoparticles, *Micro and Nanosystems*, *11* (2019), 1, pp. 34-39
[34] Kurapov, Y., *et al.*, Synthesis of Copper and Silver Nanoparticles by Molecular Beam Method, *Micro and Nanosystems, 10* (2018), 2, pp. 148-157
[35] He, J. H., Ji, F. Y., Two-Scale Mathematics and Fractional Calculus for Thermodynamics, *Thermal Science, 23* (2019), 4, pp. 2131-2133
[36] Ain, Q. T., He, J. H., On Two-Scale Dimension and Its Applications, *Thermal Science, 23* (2019), 3B, pp. 1707-1712
[37] He, J. H., Fractal Calculus and Its Geometrical Explanation, *Results in Physics, 10* (2018), Sept., pp. 272-276
[38] He, J. H., A Simple Approach to One-Dimensional Convection-Diffusion Equation and Its Fractional Modification for E Reaction Arising in Rotating Disk Electrodes, *Journal of Electroanalytical Chemistry, 854* (2019), 113565
[39] He, C. H., *et al.*, Fangzhu: An Ancient Chinese Nanotechnology for Water Collection from Air: History, Mathematical Insight, Promises and Challenges, *Mathematical Methods in the Applied Sciences*, On-line first, https://doi.org/10.1002/mma.6384, 2020

Paper submitted: April 19, 2019
Paper revised: August 28, 2019
Paper accepted: August 28, 2019